MRI measures of cerebral blood flow and cerebrovascular reactivity in the developing swine brain

J. D. Winter[1], S. Dorner[2], J. A. Fisher[3,4], K. St. Lawrence[5,6], and A. Kassner[1,7]

[1]Physiology and Experimental Medicine, The Hospital for Sick Children, Toronto, Ontario, Canada, [2]Respiratory Therapy, University Health Network, Toronto, Ontario, Canada, [3]Anaesthesiology, University Health Network, Toronto, Ontario, Canada, [4]Physiology, University of Toronto, Toronto, Ontario, Canada, [5]Imaging Division, Lawson Health Research Institute, London, Ontario, Canada, [6]Medical Biophysics, University of Western Ontario, London, Ontario, Canada, [7]Medical Imaging, University of Toronto, Toronto, Ontario, Canada

Introduction: Animal models of the immature brain enable investigations of cerebral maturation, pathology and neuronal function throughout brain development. Increasingly, the swine brain is being used as an alternative to the non-human primate for neuroimaging and neuroscience research[1]. Benefits of the swine model for developmental neuroscience include the large brain size (in contrast to rodents) and similar histology, vasculature and grey-to-white matter ratio to humans[2,3]. Moreover, swine developmental changes are similar to humans in terms of the timing of the brain growth spurt and changes in cellularity[2]. Few studies have investigated maturational changes in cerebral blood flow (CBF)[4] or CBF reserve[5,6] in swine. Therefore, the aim of this study was to characterize swine cerebrovascular development using noninvasive MRI techniques and assess its potential as an animal model for paediatric cerebrovascular disorders.

Methods: We acquired data on a 1.5 T GE Signa MRI scanner from 13 anesthetised ventilated pigs aged 1 - 12 weeks. Anesthesia was maintained with ketamine, midazolam and pancuronium constantly infused through an ear vein. To segment different tissue regions, we acquired high-resolution 3D T_1-weighted anatomical images using a fast spoiled gradient-recalled echo sequence with the following imaging parameters: TE = 4.2 ms, TR = 8.46 ms, flip angle = 20°, 3D FOV = 180 mm, and matrix size = 192 × 192 × 120.

We used a computer-controlled, model-driven prospective end-tidal targeting (MPET) system with a custom built MRI-compatible secondary circuit designed to work with any standard ventilator (RespirAct™, Thornhill Research Inc., Toronto, Canada)[7] to precisely control end-tidal CO_2 and O_2 ($P_{ET}CO_2$ and $P_{ET}O_2$) (maintained ± 1 mmHg). CBF data were acquired using FAIR ASL at a label inversion time of 1.7 s with the $P_{ET}CO_2$ fixed at 40 mmHg (controlled by the RespirAct™). We acquired 64 perfusion-weighted (ΔM) signals using background suppression and an arterial saturation pulse (850 ms post-inversion) using a single-shot spiral GE sequence. Imaging parameters included: FOV = 160 mm, matrix size = 64 × 64, slice thickness = 5 mm, slice separation = 1 mm, slices = 6, TE = 4 ms and TR = 3.75 s. For the BOLD-CVR imaging, we acquired BOLD images during four square-wave cycles of hypercapnia (~ 55 mmHg for 60 s) and normocapnia (~ 40 mmHg for 60 s). The BOLD imaging parameters included: TE = 40 ms, TR = 2 s, FOV = 160 mm, matrix size = 64 × 64, slices = 16, slice thickness = 4.5 mm, volumes = 270 and acquisition time = 9 minutes. ASL and CVR protocols were performed twice and averaged to improve SNR.

CBF images were generated from average ΔM images using a single compartmental model, as previously described[8]. For the BOLD analysis, we matched the $P_{ET}CO_2$ and BOLD MRI time courses by estimating the time delay between $P_{ET}CO_2$ and whole-brain BOLD signal. The BOLD CVR was calculated on a pixel-by-pixel basis from the slope of the regression of % MR signal with $P_{ET}CO_2$. Using the 3D anatomical volumes, we extracted mean CVR and CBF from the cortical grey matter (CGM), cortical white matter (CWM), deep GM (DGM) and deep WM (DWM) regions.

Results: The BOLD-CVR measurements exhibited a significant logarithmic increase with body weight for all regions investigated: CGM, $r = 0.87$, $p < 0.001$; CWM, $r = 0.89$, $p < 0.001$; DGM, $r = 0.86$, $p < 0.005$; DWM, $r = 0.81$, $p < 0.005$ (Figure 1). Baseline CBF in GM or WM was not related to body weight (Figure 2).

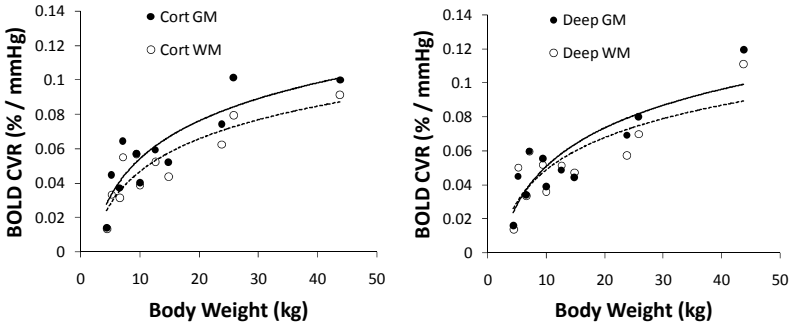

Figure 1. The BOLD cerebrovascular reactivity (CVR) in the cortical (a) and deep (b) brain regions of the developing pig. The solid (GM) and dashed (WM) lines represents the logarithmic regression lines, which were significant for all four regions ($r > 0.81$).

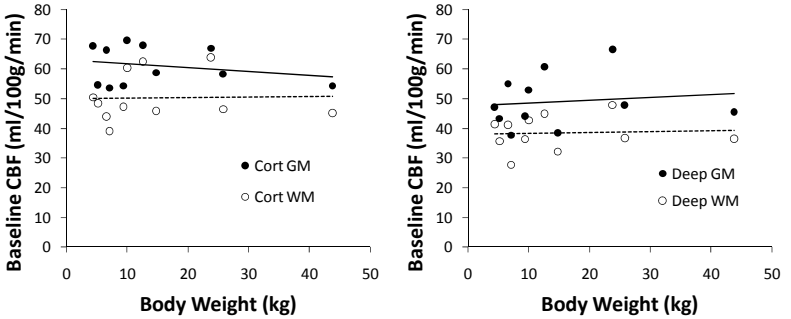

Figure 2. The ASL-based measures of cerebral blood flow (CBF) in the cortical (a) and deep (b) brain regions of the developing pig. The solid (GM) and dashed (WM) lines represents the logarithmic regression line.

Discussion: To our knowledge, this is the first study to investigate swine microvascular developmental changes using BOLD-CVR and baseline ASL-CBF. We found that CVR increased in a logarithmic fashion with maturity (body weight). This must be taken into account when assessing fMRI across different stages of development[9]. In contrast, a previous study failed to observe differences in the CVR to CO_2 between young (1 – 2 wk) and adult (6 – 10 month) pigs using radiolabeled microspheres as a measure of CBF[6]. The difference in observation may be due to the differences in what each surrogate of CBF measures.

In our study we did not actually observe CBF changes with development. This differs from humans in which a large CBF peak is observed at approximately two-years of age[10]. One previous study observed that CBF was greater in juvenile (1 - 2 month) compared with newborn (1 wk) pigs[4]; whereas, other studies also observed no CBF changes during development[5]. This discrepancy may be attributed to differences in measurement technique and anesthetics. Understanding swine cerebrovascular developmental changes will be useful for future studies utilizing the pig as a translational animal model for the study of CVR/CBF in cerebrovascular disease or fMRI during different stages of development.

References: 1. Lind NM *et al.*, Neurosci Biobehav Rev, **31**:728-51 (2007); 2. Dobbing J *et al.*, Early Hum Dev, **3**:79-83, (1979); 3. Imai H. *et al.*, J Neurosurg, **104**:123-32; 4. Nomura F *et al.*, Ann Thorac Surg, 62:115-22 (1996). 5. Kirsch JR, J. Physiol, 259:H1551-H1558 (1990); 6. Helfaer *et al.*, Am J Physio, **260**:H1482-88 (1991); 7. Prisman E, *et al.*, JMRI, **27**:185-91, (2008). 8. Koziak AM *et al.*, MRI, **26**:543-53 (2008); 9. Fang M et al., Life Sci, **78**:1197-201 (2006). 10. Wintermark M, *et al.*, Pediatrics, **113**:1642:52, (2004).